Mine Water Environ (2014) 33:97–109
DOI 10.1007/s10230-014-0277-5

TECHNICAL ARTICLE

Environmental Isotope Investigation of Groundwater in the Sarcheshmeh Copper Mine Area, Iran

Hassan Sahraei Parizi · Nozar Samani

Received: 2 December 2012 / Accepted: 5 March 2014 / Published online: 18 March 2014

Abstract Precipitation, surface, and groundwater samples were collected during 2009–2010 in the Sarcheshmeh copper mine drainage basin, Kerman Province, Iran. Groundwater samples were collected from both shallow and deep aquifers. All of the samples were analyzed for stable isotopes, deuterium (^{2}H), and oxygen-18 (^{18}O), and some were analyzed for tritium (^{3}H). The results show a more restricted range of isotopic composition in groundwater samples than in precipitation samples based on the isotopic composition of the precipitation. The isotopic composition of surface and groundwater samples plot to the right of the local meteoric water line of the Sarcheshmeh area and around the evaporation line, indicating that the groundwater within the study area originates from meteoric water that has undergone secondary evaporation before or during recharge. Tritium was below the detection limit in the deep groundwater samples while shallow groundwater samples had tritium concentrations between 1.2 and 1.7 TU, which indicates a longer residence time for deep groundwater.

Keywords Groundwater origin · Meteoric water line · Residence time · Stable isotopes

Electronic supplementary material The online version of this article (doi:10.1007/s10230-014-0277-5) contains supplementary material, which is available to authorized users.

H. S. Parizi · N. Samani
Department of Earth Sciences, College of Sciences, Shiraz University, 71454 Shiraz, Iran

N. Samani (✉)
Department of Earth Sciences, University of Waterloo, Waterloo, Canada
e-mail: samani@susc.ac.ir

Introduction

The inflow of groundwater to the pit, when mining occurs below the water table, creates many difficulties and hazards, the most important of which are: increased drilling and blasting costs, difficulties in ore handling and crushing, decreased machinery life, slope instability, degradation of water quality, and environmental problems (Sahraei Parizi and Samani 2012). Therefore, management of groundwater and planning of appropriate dewatering systems are imperative requirements for safe, sustainable, and cost effective mining below the water table. Adequate management of groundwater (Fantong et al. 2010; Matter et al. 2005) and controlling groundwater inflows to the mine cuttings (Morton and Mekerk 1993) requires good understanding of the sources of recharge and the major groundwater flow paths. Establishment of the source and flow paths of groundwater in hard rock aquifers with complex lithology is difficult; isotopic studies can provide useful complementary information in such aquifers (Girard et al. 1997 after Geirnaert et al. 1984).

The stable isotopes of water, deuterium (^{2}H) and oxygen-18 (^{18}O) are indicators of conditions present at the time and place of groundwater recharge (Faure 1986), while the radioactive isotope, tritium (^{3}H), can be used to assess the residence time of groundwater. These rare components of the water molecule (Goni 2006) have been widely used as essential naturally occurring tracers to evaluate the origin and the residence times of water resources and to trace the flow paths of groundwater (Abu-Jaber and Kharabsheh 2008; Acheampong and Hess 2000; Chen et al. 2006; Cloutier et al. 2006; Edmunds et al. 1992; Leybourne and Goodfellow 2007; Njitchoua et al. 1997; Ortega-Guerrero 2003; Wassenaar et al. 2011).

Analysis of groundwater origin usually involves comparing ^{2}H and ^{18}O values of groundwater samples of the study area to world precipitation data, presented by Craig (1961) as the global meteoric water line (GMWL):

$$\delta^{2}H = 8\delta^{18}O + 10 \quad (1)$$

and against the local precipitation data, represented as the local meteoric water line (LMWL). The LMWLs are different from the GMWL, both in their slopes and intercepts. These differences result from the fact that the meteoric water line of a specific region is controlled by local factors, which are specific to the climate of that region, such as the origin of the water vapor, the temperature of condensation, and secondary evaporation of precipitation. Slopes flatter than 8 indicate modification due to secondary evaporation during rainfall, which is greatest for light rains (Clark and Fritz 1997; Friedman et al. 1962). This effect is restricted to rainfall events because snow does not evaporate as it falls through the atmosphere (Rose et al. 1997).

The intercept of the meteoric water line (or the d-excess value), which is defined as:

$$d = \delta^{2}H - 8\delta^{18}O \quad (2)$$

varies regionally due to variations in humidity, wind speed, and sea surface temperature during primary evaporation. Large d-excess values indicate low-humidity conditions in the source area of the water vapor.

Groundwater stable isotope values that plot along the LMWL were compared to local precipitation mean values to determine if groundwater was derived from recent local recharge or from water that recharged the aquifer under climatic conditions different than the present (Hamed et al. 2011). Deviations from the LMWL indicate modification of the groundwater isotopic composition by processes such as evaporation, water–rock interactions, exchange with the surrounding environment, or mixing of different water types. Depending on the altitude effect on the isotopic composition of precipitation, isotopes may be used to identify waters coming from different potential recharge sources (Leontiadis et al. 1996).

Tritium (^{3}H) can be used to indicate whether the recharge is recent or older and to obtain a preliminary interpretation of relative groundwater residence times (Abbott et al. 2000; Girard et al. 1997 after Geirnaert et al. 1984). Tritium is the only radioactive isotope suitable for estimating ages of groundwater (Axel 2006), and due to its short half-life (12.43 years), tritium is ideal for dating young groundwater (Kazemi et al. 2006). Interpretation of tritium data is difficult due to the effects of the atomic bomb testing peak period (Engle et al. 2008) and due to the mixing of waters with different residence times in aquifers, but tritium data can be used as an indicator of the relative residence times of different groundwater resources.

The geology and hydrogeology of the Sarcheshmeh area are complex due to the presence of different rock types that were intruded during different magmatic phases and the effects of alteration and geological structures. In such a complex area, where conventional hydrogeological methods may fail to clarify the groundwater status, complementary studies such as hydrochemical and isotopic studies can provide useful information about the groundwater and its residence time.

The Sarcheshmeh area groundwater and the main processes responsible for the hydrochemical evolution of this water have been explained previously (Sahraei Parizi and Samani 2012). The present study analyses the isotopes of water in the study area to complement the previous work by defining the origin, age, and recharge zone of the groundwater. First, the LMWL and the evaporation line of the Sarcheshmeh area were established. Then the origin and the residence times of groundwater in the area were evaluated. The site measurements indicated that artesian groundwater in the area was warmer than expected, so the source of this warming was also assessed. Lastly, these analyses were used to develop a conceptual groundwater model of the study area that can be used to design a long-term dewatering scheme for the Sarcheshmeh copper mine pit. LMWLs have been defined only for a small number of regions in Iran (Khademi et al. 1997; Mohammadi 2006; Mohammadzadeh 2010; Mohammadzadeh and Ebrahimpoor 2012) and, as far as we know, the LMWL established in this study is the first LMWL in southeastern Iran. This LMWL can be used as a reference line for future isotopic studies in this region or at least in Kerman province.

Study Area

The Sarcheshmeh porphyry copper deposit is a world-class copper deposit which, based on exploration data and recent evaluation, has a reserve of more than 1,500 Mt (SRK 2011). This deposit is located in southern Iran in a NW trending mountain belt known as Band-e-Mamzar (Fig. 1). This mountain belt is flanked to the north and south by the broad Rafsanjan and Sirjan alluvial plains, respectively. The highest peak of the mountainous area has an elevation of about 3,200 m (elevations are relative to the mine datum, which is 125.97 m above the Universal Transverse Mercator (UTM) datum); the north alluvial plain has elevations around 1,550 m and the mean elevation of the south plain is about 1,650 m.

Large scale open pit mining was started up in 1974 at Sarcheshmeh by the National Iranian Copper Industries Company (NICICO). Presently, the pit has an oval shape about 3,000 m long and 2,000 m wide (Fig. 2), and drains a basin with an area about 21 km^{2}. Ground surface

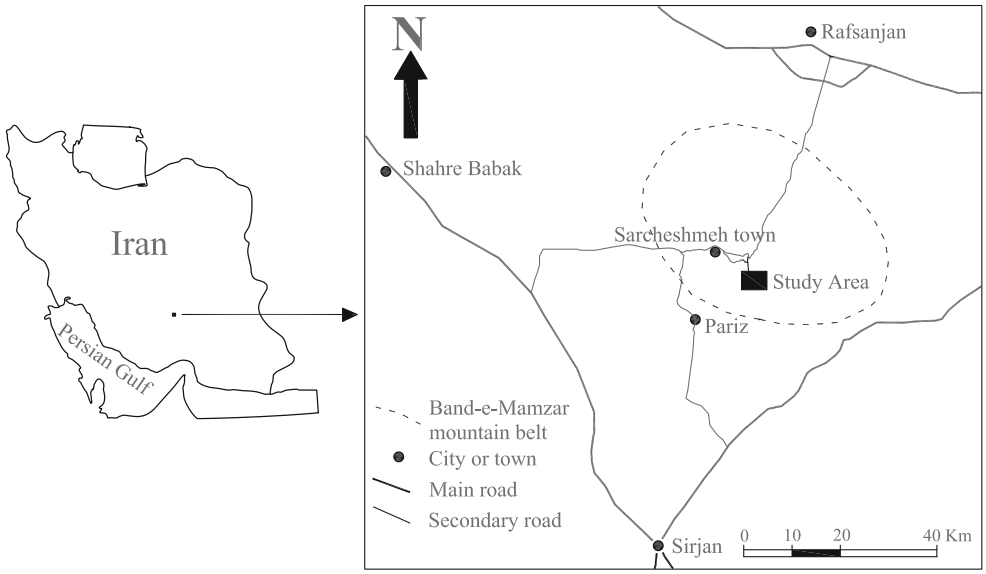

Fig. 1 Location of the study area

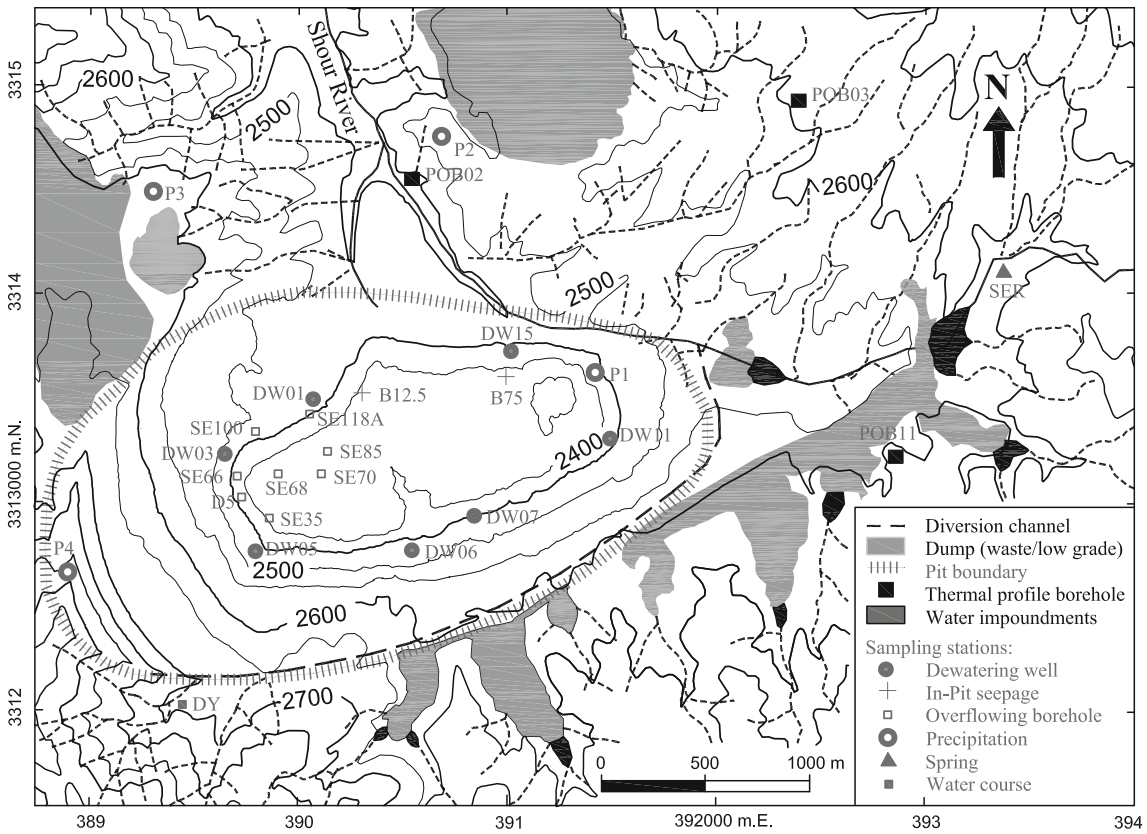

Fig. 2 Location of pit and sampling points in the map of study area (topographic contours are in meters and grid northings and eastings based on UTM)

elevations around the perimeter of the Sarcheshmeh pit ranges between 2,925 m in the western wall to 2,500 m in the northern wall. The deepest part of the pit floor presently (September, 2012) has an elevation of 2,350 m.

Figure 3 is a geological map of the study area. The country rock mainly consists of Eocene andesites, which host various intrusives, with the late Tertiary Sarcheshmeh porphyry stock, with a granodioritic composition, being the

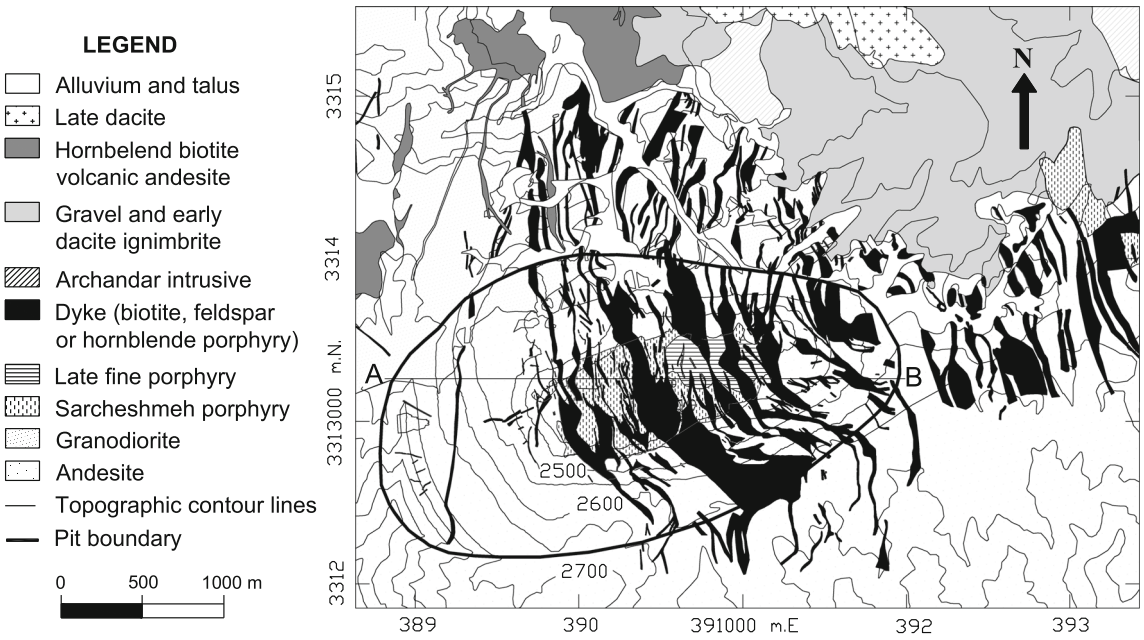

Fig. 3 Geological map of the Sarcheshmeh copper mine area (after Sahraei Parizi and Samani 2012)

largest. The mineralization at Sarcheshmeh is associated with this porphyry stock (Shahabpour 1982). A Pliocene fine-grained porphyritic rock with granodioritic composition, called the late fine porphyry, has been emplaced in the central part of the deposit, displacing the older rocks (Shahabpour and Kramers 1987, and is associated with weak mineralization.

All of the above-mentioned rock types have been cut by three sets of steeply dipping dykes with a general trend of N-NW to S-SE. These dyke sets, which include hornblende porphyry, feldspar porphyry, and biotite porphyry dykes, have a granodioritic composition and are weakly altered (Sahraei Parizi and Samani 2012).

Hydrological and Hydrogeological Setting

The Sarcheshmeh area is located in a semiarid region with mean annual precipitation about 400 mm and a mean annual evapotranspiration of about 1,170 mm. The temperature of the area ranges between −22 and +35 °C annually. Surface runoff that occurs during December through May (concurrent with the most precipitation and snow melting in the region), flows toward the pit in the lowest western part of the Sarcheshmeh basin (Sahraei Parizi and Samani 2012). A fraction of the surface runoff ponds behind the waste dumps that have filled the end part of the water courses (at the border of the pit) and the remaining runoff, plus additional flow from seepage out of the dumps, flows into a diversion channel and exits the Sarcheshmeh basin to the north into the Shour River (Fig. 2).

The aquifers of the Sarcheshmeh area are formed in the andesite host rock and in two granodioritic stocks that are structurally weak and have undergone large-scale fracturing during and after mineralization. The transmissivity of these aquifers ranges between 50 and 300 m^2/day and their storage coefficients range from 0.0005 to 0.004 (Sahraei Parizi and Samani 2012). In contrast, the compact and fresh dykes with a N–NW trend (Fig. 3) appear to be effective barriers to groundwater flow and divide the basin into many small individual aquifers. Mining activities such as drilling, blasting, and mine excavation can create hydraulic connections between these individual aquifers in the mine area, whereas in other undisturbed areas, these aquifers remain disconnected. Figure 4 shows a W-E hydrogeological cross section through the pit (the location of this section is presented in Fig. 3). Based on this figure, two aquifers with distinct water levels are formed on either side of an inclined hornblende porphyry dyke (IHPD), which is located under the western wall of the pit. We refer to these aquifers as the western and eastern aquifers. As a result of the hydraulic behavior of this dyke and other similar dykes, most of the inclined diamond drill exploration boreholes, which were drilled during 2009 and 2010 in the western wall of the Sarcheshmeh pit, encountered artesian conditions, resulting in overflowing wells. Some of these boreholes are shown in Fig. 4.

Methodology

Rain and snow samples of all precipitation events greater than 10 mm were collected during the rainy season of

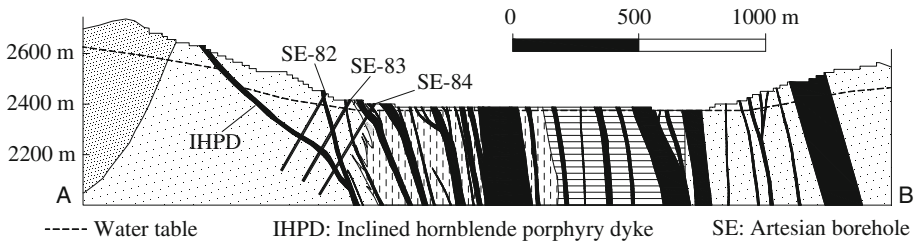

Fig. 4 Hydrogeological cross sections through the pit (modified after Sahraei Parizi and Samani 2012)

2009–2010 at four stations with different elevations in the study area. Rain water samples were collected by allowing water to accumulate in a funnel with a diameter of about 40 cm, and drip into a polyethylene bottle through a U-shaped hose. The U-shaped hose was designed to remain filled with water after a precipitation event, thus protecting the water sample in the collection bottle from evaporation and associated isotopic enrichment. Snow samples were prepared by collecting all of the snow that accumulated in the funnel and then allowing it to melt in sealed containers at room temperature. All samples were collected within 15 h of each precipitation event in order to minimize the alteration of isotopes by evaporation.

Groundwater samples were collected from seven dewatering wells (each 150 m deep, which were located in the pit and pumped continuously), eight overflowing artesian boreholes with depths mostly greater than 300 m, one spring in the eastern part of the Sarcheshmeh basin (Seridon spring, SER) and two seepage points in the pit. In addition, one surface runoff sample was collected from the Deh-Yahya (DY) water course in the southwestern part of the basin. The locations of all sampling stations are shown in Fig. 2. Samples of all dewatering wells and the SER spring, in addition to two overflowing artesian boreholes (D5 and SE35) and one of the seepage points (B75), were collected in both wet (February 2010) and dry (September 2010) seasons, whereas the other sampling stations were sampled either in February or in September 2010. In order to develop the evaporation line of the Sarcheshmeh area, a class A evaporation pan was installed in the meteorological station of the Sarcheshmeh pit (P2, Fig. 2) and filled with water. Intermittent sampling from the water of this pan was performed until almost all of the water was evaporated.

The samples for stable isotope analyses were stored in 30 ml glass bottles with poly-sealed lids and the 8 samples for tritium analysis (from 3 dewatering wells, 3 overflowing artesian boreholes, 1 spring, and 1 surface water) were stored in 250 ml polyethylene bottles. Both sets of samples were preserved in a cool and dark place until they arrived in the laboratory.

All isotopic analyses were performed at the Environmental Isotope Laboratory of the University of Waterloo (Canada). Oxygen (^{18}O) was determined by CO_2 equilibration using standard procedures based on the principals of Epstein and Mayeda (1953). The deuterium determination was performed on hydrogen gas produced from water reduced on hot chromium, using procedures outlined by Drimme et al. (2001).

The results of oxygen and hydrogen stable isotope analyses were expressed in per mil units using the δ notation relative to the VSMOW (Vienna standard mean oceanic water), in which:

$$\delta = ((R/R_{VSMOW}) - 1)1000 \quad (3)$$

with R and R_{VSMOW} being the $^{18}O/^{16}O$ or the $^{2}H/^{1}H$ ratio of the sample and standard, respectively. The analytical reproducibility is ±0.2 ‰ for $\delta^{18}O$ and ±0.8 ‰ for $\delta^{2}H$.

Tritium samples were prepared by electrolytic enrichment and analyzed by the liquid scintillation counting method. Tritium concentrations were expressed in tritium units (1 TU = 3.24 pCi/ml = 1 tritium atom per 1,018 hydrogen atoms). The analytical precision was ±0.8 TU.

In order to investigate the cause of higher water temperatures in the overflowing boreholes with respect to other water resources of the area, monthly water temperature surveys of three artesian boreholes and three dewatering wells were completed during Nov. 2009 to May 2010. In the dewatering wells, temperature was measured at the static water table (about 24 h after the shutdown of the pumps), whereas the temperature of the artesian boreholes was measured at their outlets.

Results

Stable Isotopes of Precipitation

The $\delta^{2}H$ and $\delta^{18}O$ values of 32 precipitation samples are presented in Table 1. The $\delta^{18}O$ values of precipitation samples range between −10.97 and −1.15 ‰ and those of $\delta^{2}H$ vary from −66.13 to +5.30 ‰, with weighted mean values of −6.03 and −27.69 ‰ for $\delta^{18}O$ and $\delta^{2}H$, respectively. A least squares regression of the precipitation stable isotope data resulted in the following LMWL for the Sarcheshmeh area (Fig. 5):

$$\delta^{2}H = 7.25\delta^{18}O + 15.22 (r^{2} = 0.93) \quad (4)$$

Table 1 Isotopic data of precipitation in the Sarcheshmeh area

Station ID	Sample ID	Sampling date	$\delta^{18}O$ (‰)	$\delta^{2}H$ (‰)	d-excess (‰)
P1	P1-1	29/11/2009	−1.15	2.59	11.83
	P1-2	09/12/2009	−9.17	−48.39	24.97
	P1-3	20/12/2009	−6.70	−32.20	21.44
	P1-4	26/01/2010	−2.29	5.30	23.60
	P1-5	06/02/2010	−5.07	−15.71	24.83
	P1-6	26/02/2010	−5.15	−30.30	10.93
	P1-7	28/02/2010	−4.76	−21.40	16.71
	P1-8	13/03/2010	−5.90	−27.61	19.59
P2	P2-1	29/11/2009	−3.73	−8.52	21.33
	P2-2	09/12/2009	−9.80	−54.12	24.32
	P2-3	20/12/2009	−7.50	−38.48	21.51
	P2-4	26/01/2010	−2.98	2.06	25.93
	P2-5	06/02/2010	−5.86	−22.04	24.81
	P2-6	26/02/2010	−5.36	−30.80	12.10
	P2-7	28/02/2010	−5.15	−23.74	17.42
	P2-8	13/03/2010	−4.41	−21.85	13.44
P3	P3-1	29/11/2009	−3.22	−10.80	14.96
	P3-2	09/12/2009	−9.92	−57.14	22.26
	P3-3	20/12/2009	−5.81	−28.21	18.24
	P3-4	26/01/2010	−3.12	−0.08	24.90
	P3-5	06/02/2010	−5.90	−20.39	26.81
	P3-6	26/02/2010	−7.06	−39.13	17.34
	P3-7	28/02/2010	−5.94	−24.04	23.46
	P3-8	13/03/2010	−5.30	−23.55	18.86
P4	P4-1	29/11/2009	−4.59	−17.62	19.10
	P4-2	09/12/2009	−10.97	−66.13	21.63
	P4-3	20/12/2009	−6.65	−42.71	10.53
	P4-4	26/01/2010	−1.87	−4.46	10.52
	P4-5	06/02/2010	−6.77	−34.00	20.17
	P4-6	26/02/2010	−8.93	−46.29	25.15
	P4-7	28/02/2010	−5.94	−28.80	18.73
	P4-8	13/03/2010	−5.26	−26.04	16.03

Stable Isotopes of Evaporation Pan Water

Table 2 shows the results of isotopic analyses of nine water samples taken periodically from the remaining water in the evaporation pan, as previously described. The data shows enrichment of pan water in heavy isotopes with time; $\delta^{2}H$ changed from −34.37 ‰ in the primary water to 157.27 ‰ in the final sample of remaining water and $\delta^{18}O$ was enriched from −5.7 to 38.55 ‰. The best line fit for the data (Fig. 6) was:

$$\delta^{2}H = 4.22\delta^{18}O - 14.85 \quad (5)$$

which is assumed to be the evaporation line of the Sarcheshmeh region.

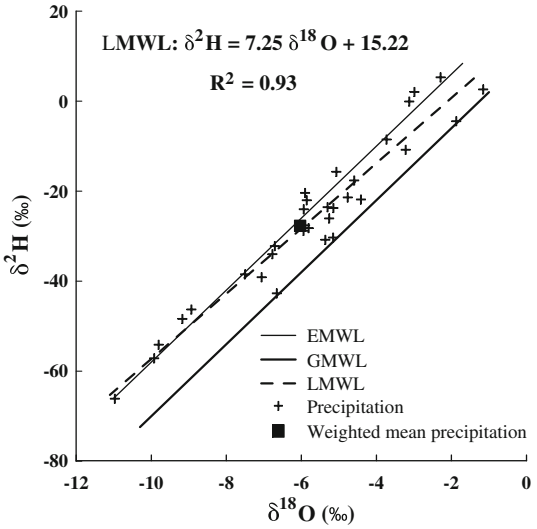

Fig. 5 The isotopic composition of precipitation and LMWL of the Sarcheshmeh region

Table 2 Isotopic data of remaining water in the evaporation pan, Sarcheshmeh area

Sample ID	Sampling date	Remaining water (%)	$\delta^{18}O$ (‰)	$\delta^{2}H$ (‰)
E1	13/06/10	100	−5.70	−34.37
E4	16/06/10	78	−1.57	−18.05
E6	18/06/10	68	2.44	−7.31
E8	20/06/10	57	5.18	3.56
E10	22/06/10	31	15.18	46.46
E11	23/06/10	19	22.37	77.83
E12	24/06/10	13	27.18	99.06
E13	25/06/10	6	35.49	129.77
E14	26/06/10	1	38.55	157.26

Stable Isotopes of Surface and Groundwater Samples

The $\delta^{2}H$ and $\delta^{18}O$ values of one surface water and 29 groundwater samples are presented in Table 3. Groundwater samples are sub-divided into shallow and deep groups. The shallow group includes samples from the dewatering wells in addition to samples of in-pit seepages and the Seridon spring (SER). All of these stations discharge from the eastern aquifer. The overflowing boreholes form the deep groundwater group discharge from the western aquifer.

In the deep groundwater samples, $\delta^{18}O$ values averaged −6.34 ‰ and ranged from −6.65 to −5.67 ‰; the variation of $\delta^{2}H$ ranged from −35.77 to −31.98 ‰, with an average of −33.91 ‰. The isotopic composition of the dewatering wells (shallow groundwater) ranged for $\delta^{18}O$ from −6.60 to −5.45 ‰ and from −35.55 to −30.49 ‰ for $\delta^{2}H$, with averages of −5.99 and −32.97 ‰ for $\delta^{18}O$

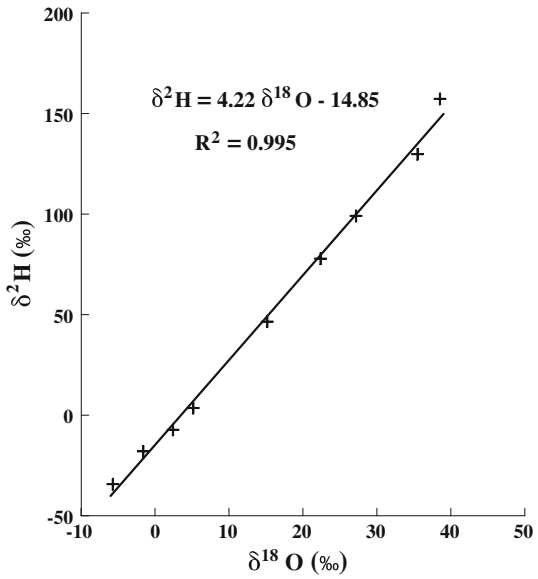

Fig. 6 Evaporation line of the Sarcheshmeh region

and δ^2H, respectively. Samples taken from the two in-pit seepages had $\delta^{18}O$ values ranging from −6.23 to −5.66 ‰, with an average of −5.95 ‰. The δ^2H values of these samples ranged between −32.74 ‰ and −30.52 ‰, with an average value of −31.93 ‰. The $\delta^{18}O$ and δ^2H of two samples taken from the SER spring have average values of −5.84 and −30.01 ‰ and show no significant difference between wet and dry seasons. The DY water course had the most enriched water sample, with $\delta^{18}O$ and δ^2H values of −4.67 and −26.55 ‰, respectively. All $\delta^{18}O$ and δ^2H values of groundwater samples are plotted in Fig. 7 against the LMWL of the Sarcheshmeh region, and provide some indication of the origin and the recharge processes of the groundwater.

To evaluate the relative residence time of groundwater, 8 water samples, chosen to represent both shallow and deep groundwater, were analyzed for enriched ^3H (Table 3). Four samples, with tritium activities between 1.2 and 1.7 TU, characterize the shallow groundwater of the study area and three samples with tritium activities below the detection limit (0.8 TU), characterize deep groundwater. The tritium activity of the DY sample, which is assumed to represent present day recharge water of the area, is 3.4 TU.

Groundwater Temperature Data

Figure 8 shows monthly temperature of water in three overflowing boreholes (D5, SE35, and SE70) and three dewatering wells (DW01, DW06, and DW11), in addition to air temperature during 7 months (November 2009 to May 2010). As this figure shows, the water of artesian overflowing boreholes (deep groundwater) is 6–9 °C warmer than the shallow groundwater in the dewatering wells.

Discussion

Local Meteoric Water Line

According to Fig. 5, the LMWL of the Sarcheshmeh area is located above the GMWL defined by Eq. 1 (Craig 1961) and below the eastern Mediterranean meteoric water line (EMWL), as defined by Gat and Carmi (1970):

$$\delta^2H = 8\delta^{18}O + 22 \quad (6)$$

This line is comparable with some of the LMWLs defined for different regions of Iran and neighboring countries (supplementary Table S1, available in the online version of this paper). The slope of the Sarcheshmeh LMWL was less than Craig's GMWL, demonstrating that the rainfall of the area experiences evaporation. All of the d-excess values of the precipitation samples of the Sarcheshmeh area, which range between 10.52 and 26.81 ‰ (Table 1), are greater than the global mean d-excess of 10 ‰. Since most of the air mass that enters the study area is Mediterranean in origin, the large d-excess value of the precipitation was expected.

Evaporation Line

Equation (5) shows that the slope of the evaporation line of the Sarcheshmeh area is about 4. According to Gat (1971), slopes close to 4 are specific to areas with a relative humidity of $\approx$25 %. Since the study area is located in a semiarid region, the slope of the evaporation line agrees with the environmental conditions.

Origin of Groundwater

The entire data set plots to the right-hand side of the LMWL and around the evaporation line (Fig. 7). The clustering of water samples around the evaporation trend line and near to the LMWL indicates a common origin for both shallow and deep groundwater, namely precipitation. The location along the evaporation line of the DY ephemeral water course point (shown as the surface water point in Fig. 7), which directly originates from rainfall or snow melt, supports the assessment that meteoric water was the source of the shallow and deep groundwater. However, the DY sample shows more isotopic enrichment due to higher degrees of evaporation. The lower d-excess values of groundwater samples with respect to precipitation (Tables 1, 3) also indicate secondary isotopic enrichment caused by evaporation (Chen et al. 2006).

Although all of the shallow and deep groundwater samples lie around the evaporation trend line, the deep artesian boreholes samples lie closer to the meteoric water

Table 3 Isotopic data of surface and groundwater samples of the Sarcheshmeh area

Sample type	Station type	Sample ID	Sampling date	$\delta^{18}O$ (‰)	$\delta^{2}H$ (‰)	d-excess (‰)	^{3}H (TU)
Shallow groundwater	Dewatering well	DW01-1	10/02/2010	−5.47	−30.70	13.06	
		DW01-2	13/09/2010	−6.60	−35.49	17.32	1.2
		DW03-1	10/02/2010	−5.87	−32.51	14.43	
		DW03-2	13/09/2010	−6.26	−35.55	14.52	
		DW05-1	10/02/2010	−5.45	−32.18	11.38	
		DW05-2	13/09/2010	−6.23	−33.55	16.31	
		DW06-1	10/02/2010	−6.16	−32.90	16.40	
		DW06-2	13/09/2010	−6.05	−31.99	16.41	1.7
		DW07-1	10/02/2010	−5.72	−32.50	13.24	
		DW07-2	13/09/2010	−5.85	−30.49	16.35	
		DW11-1	17/02/2010	−5.88	−32.09	14.96	
		DW11-2	13/09/2010	−6.27	−34.76	15.41	1.3
		DW15-1	10/02/2010	−5.99	−32.35	15.59	
		DW15-2	13/09/2010	−6.12	−34.47	14.52	
	In-pit seepage	B12.5-1	17/02/2010	−5.66	−32.52	12.80	
		B75-1	10/02/2010	−6.23	−32.74	17.13	
		B75-2	13/09/2010	−5.95	−30.52	17.06	
	Spring	SER-1	10/02/2010	−5.85	−29.60	17.17	
		SER-2	13/09/2010	−5.84	−30.43	16.31	1.7
Deep groundwater	Overflowing borehole	D5-1	10/02/2010	−5.67	−31.98	13.38	<0.8
		D5-2	13/09/2010	−6.45	−33.53	18.11	
		SE100-1	12/09/2010	−6.40	−33.94	17.24	
		SE118A-1	12/09/2010	−6.48	−35.54	16.30	
		SE35-1	24/02/2010	−6.32	−32.79	17.73	
		SE35-2	13/09/2010	−6.65	−35.77	17.43	<0.8
		SE66-1	10/02/2010	−6.58	−33.10	19.53	
		SE68-1	12/09/2010	−5.90	−32.26	14.94	
		SE70-1	10/02/2010	−6.54	−35.62	16.71	<0.8
		SE85-1	17/02/2010	−6.45	−34.56	17.02	
Surface Water	Water course	DY-1	10/02/2010	−4.67	−26.55	10.80	3.4

line and therefore, according to Engle et al. (2008), have undergone less evaporation before or during the recharge process.

Recharge Areas of Groundwater

The weighted mean $\delta^{2}H$ values in precipitation at four sampling stations were plotted against elevation (Fig. 9). The precipitation at higher elevations is more depleted in isotopic composition, reflecting the fact that decreasing air temperature with increasing elevation causes isotopic fractionation, so that at higher elevations, precipitation is isotopically depleted in ^{2}H and ^{18}O (Clark and Fritz 1997; Leybourne et al. 2006). This effect can be used to identify potential groundwater recharge sources (Lee et al. 1999; Leontiadis et al. 1996).

Based on a best-fit linear interpretation of the relationship for weighted mean values of $\delta^{2}H$ of precipitation versus elevation, the following equation was developed to estimate recharge elevation of groundwater of the Sarcheshmeh basin:

$$E = -24.62\delta^{2}H + 1929.3 \quad (7)$$

where E is the mean recharge elevation (m). Since the isotopic composition of groundwater is affected by evaporation, the original isotopic values of the recharged water (prior to evaporation) must be determined in order to estimate the recharge elevation points of groundwater. These values can be inferred by determining the slope of the evaporation trend line (Clark and Fritz 1997). The original values of $\delta^{18}O$ and $\delta^{2}H$ were determined by calculating the intersection of the evaporation line with the LMWL (Table 4). The original $\delta^{18}O$ and $\delta^{2}H$ values of the groundwater samples ranged from −7.93 to −6.60 ‰ and from −42.40 to −32.64 ‰, respectively. The mean of the original $\delta^{18}O$ and $\delta^{2}H$ values were −7.36 and −38.18 ‰,

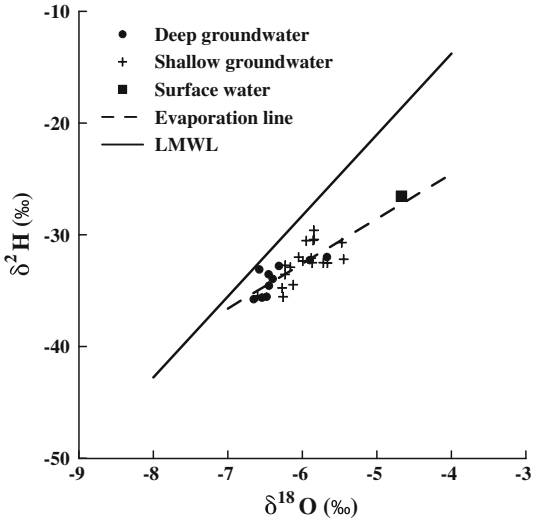

Fig. 7 Plot of δ^2H versus $\delta^{18}O$ of water samples of the study area against the LMWL and evaporation line

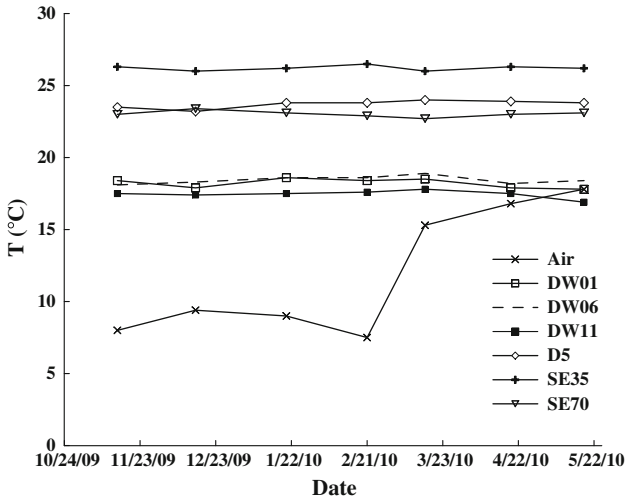

Fig. 8 Time variation of air and water temperatures in some of the artesian boreholes and dewatering wells

respectively (Table 4). The original isotopic values of the groundwater samples were depleted in both $\delta^{18}O$ and δ^2H, relative to the weighted mean values of local precipitation (−6.03 and −27.69 ‰, respectively; Fig. 5). This discrepancy in isotopic content can be attributed to the lower condensation temperature of the precipitation that contributes to the recharge, which can be due to an altitude effect (recent high altitude recharge) or to a paleo-climatic effect (recharge under colder climatic conditions than at present) (Hamed et al. 2011). However, the presence of tritium (^3H) in shallow groundwater samples (Table 3) rejects the paleo-water origin, due to the short half-life of tritium; hence the groundwater of the study area most likely originated from high altitude recharge from recent

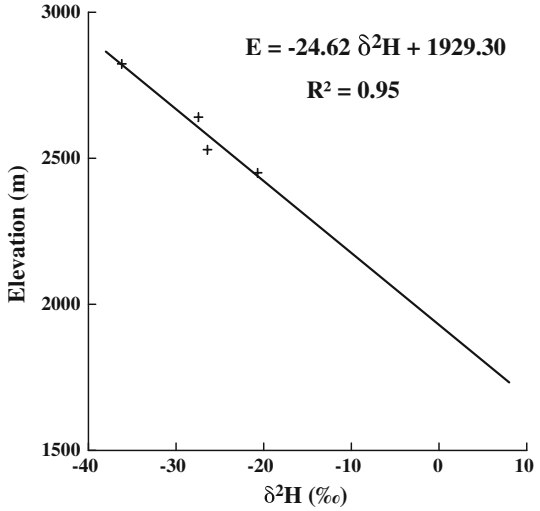

Fig. 9 Correlation between δ^2H of precipitation and elevation

precipitation. The approximate recharge elevations of the groundwater were calculated by substituting the corrected δ^2H values into Eq. (7). The calculated recharge elevations, ranging between 2,730 and 2,970 m above mean sea level with a mean value of 2,870 m (Table 4), indicate that most of the recharged water comes from high altitudes.

Residence Time of Groundwater

The assumption of the DY sample as an indicator of recent recharge reveals that the shallow groundwater has a maximum residence time of two decades, and is essentially modern in origin. On the other hand, the tritium-free samples of the deep groundwater group indicate an older origin for these waters or that they result from significant mixing of groundwater. However, as mentioned in the previous sections, the position of these water samples on the δ^2H versus $\delta^{18}O$ diagram (Fig. 7), and the similarity of their stable isotope values with the shallow groundwater, suggests that the deep groundwater is meteoric in origin, with a likely residence time of more than a few decades.

Heating Source of Deep Groundwater

Based on the above-mentioned isotopic studies, both the shallow and deep groundwater have meteoric origins and are recharged from high elevations. Therefore, an inter-aquifer factor should be the cause of increased deep groundwater temperatures. According to Gupta and Ray (2007) the release of heat due to the cooling of the earth (or the geothermal gradient) and the heat produced by radioactivity appear to be primarily responsible for such temperature distributions. Exothermic chemical reactions can also produce some heat.

Table 4 Measured and original isotopic data of groundwater samples and their calculated recharge elevation

Sample ID	Measured $\delta^{18}O$ (‰)	Measured $\delta^{2}H$ (‰)	Original $\delta^{18}O$ (‰)	Original $\delta^{2}H$ (‰)	Recharge elevation (m)
DW01-1	−5.47	−30.70	−7.47	−38.58	2,880
DW03-1	−5.87	−32.51	−7.47	−39.15	2,890
DW05-1	−5.45	−32.18	−7.93	−42.40	2,970
DW06-1	−6.16	−32.90	−7.23	−37.18	2,840
DW07-1	−5.72	−32.50	−7.66	−40.53	2,930
DW11-1	−5.88	−32.09	−7.34	−37.98	2,860
DW15-1	−5.99	−32.35	−7.28	−37.58	2,850
B12.5-1	−5.66	−32.52	−7.76	−41.20	2,940
B75-1	−6.23	−32.74	−7.12	−36.32	2,820
SER-1	−5.85	−29.60	−6.60	−32.64	2,730
D5-1	−5.67	−31.98	−7.56	−39.68	2,910
SE100-1	−6.40	−33.94	−7.25	−37.40	2,850
SE118A-1	−6.48	−35.54	−7.67	−40.55	2,930
SE35-1	−6.32	−32.79	−6.99	−35.58	2,800
SE66-1	−6.58	−33.10	−6.77	−33.88	2,760
SE68-1	−5.90	−32.26	−7.36	−38.18	2,870
SE70-1	−6.54	−35.62	−7.62	−40.05	2,920
SE85-1	−6.45	−34.56	−7.38	−38.35	2,870
Mean	−6.03	−32.77	−7.36	−38.18	2,870

Sahraei Parizi and Samani (2012) showed that oxidation of pyrite, which is an exothermic reaction, is the most important process responsible for the hydrochemical evolution of water in the Sarcheshmeh area. Fe^{2+}, SO_4^{2-}, and H^+ are the principal products of pyrite oxidation. If the heating of deep groundwater was due to this process, these waters would have higher concentrations of SO_4^{2-} with respect to shallow groundwater. This is not the case (Table 5), indicating that pyrite oxidation does not play any significant role in the heating of the deep groundwater in the study area.

Since there is no indication of radioactive elements and radioactivity in the Sarcheshmeh area, the geothermal gradient is the most likely factor responsible for the heating of the deep groundwater. Figure 10 shows the depth variation of temperature in three observation boreholes (Fig. 2). The geothermal gradient in the study area varies between 2.7 and 3.8 °C/100 m, with an average of 3.2 °C/100 m. With this average geothermal gradient, 6–9 °C warming could occur over a depth increase of about 180–280 m. Table 6 shows the elevation of the static water table in dewatering wells (where their water temperatures were measured), the level at which the exploration boreholes start overflowing, and the average temperature of water in these wells and boreholes. Based on this table, the depth difference between the static water table of

Table 5 Concentration of SO_4^{2-} in water samples

Station ID	Station type	SO_4^{2-} (mmol/l)
DW01	Dewatering well	1.54
DW06	Dewatering well	5.92
DW11	Dewatering well	7.94
D5	Overflowing borehole	4.53
SE35	Overflowing borehole	6.44
SE70	Overflowing borehole	0.61

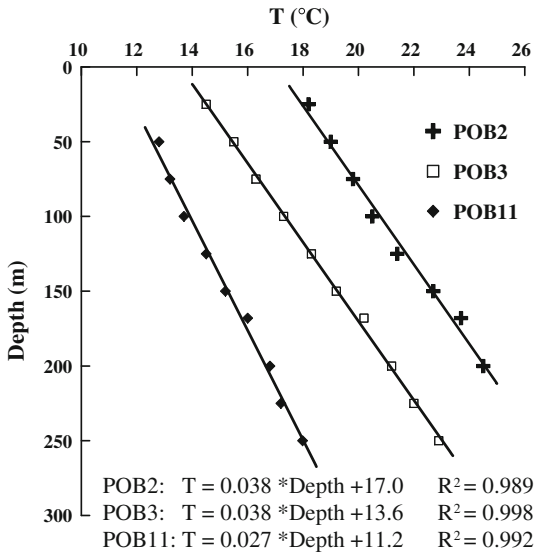

Fig. 10 Depth variations of temperature within three boreholes in the Sarcheshmeh area

Table 6 Characteristics of selected overflowing boreholes and dewatering wells

Station ID	Collar elevation (m)	Elevation of static water Table (m)	Elevation of Artesian level (m)	Mean water temperature (°C)
D5	2,453.10	–	2,154.95	23.7
SE35	2,428.19	–	2,092.99	26.2
SE70	2,426.70	–	2,241.40	23.0
DW01	2,451.84	2,392.00	–	18.2
DW06	2,452.75	2,391.09	–	18.4
DW11	2,436.99	2,369.16	–	17.4

dewatering wells and the artesian level of overflowing boreholes can account for the observed differences in temperature. Therefore, the normal geothermal gradient of the area is the probable heating source in the artesian boreholes.

Conceptual Model of Groundwater Flow

As discussed in the previous sections, high altitude parts of the basin play an important role in the recharge of both shallow and deep groundwater systems. Snow, which is the dominant form of precipitation in the high altitudes, freezes due to persistent low temperatures during winter and forms a snowpack (in some cases, until summer). Sublimation and vapor exchange within the snowpack in addition to an exchange between the snow and melt water are the two main processes that modify the isotopic composition of snowpack (Clark and Fritz 1997). The consequence of this modification is isotopic enrichment similar to that of evaporation. A fraction of this isotopically-enriched water infiltrates to recharge the groundwater and another part forms the surface runoff of the area, which flows down-gradient and is locally impounded behind the waste dumps (Fig. 11).

As Fig. 11 illustrates, the west aquifer, which supplies the water of the artesian boreholes, is mainly recharged by melt water from the high altitudes, whereas the east aquifer is recharged by melt water, runoff, and ponded water. Although evaporation can alter the isotopic composition of all components of the recharge water, it has a greater effect on the runoff and ponded water. As a result of this process, the shallow groundwater samples show higher degrees of isotopic enrichment with respect to the deep groundwater samples (Fig. 7).

The higher temperature of the artesian borehole water relative to the dewatering wells can also be explained by the conceptual model (Fig. 11). Level 1 in Fig. 11 represents a typical elevation of the water table in the east aquifer where the water temperature in the dewatering wells was measured, while level 2 represents the level at which exploration boreholes start overflowing (and hence

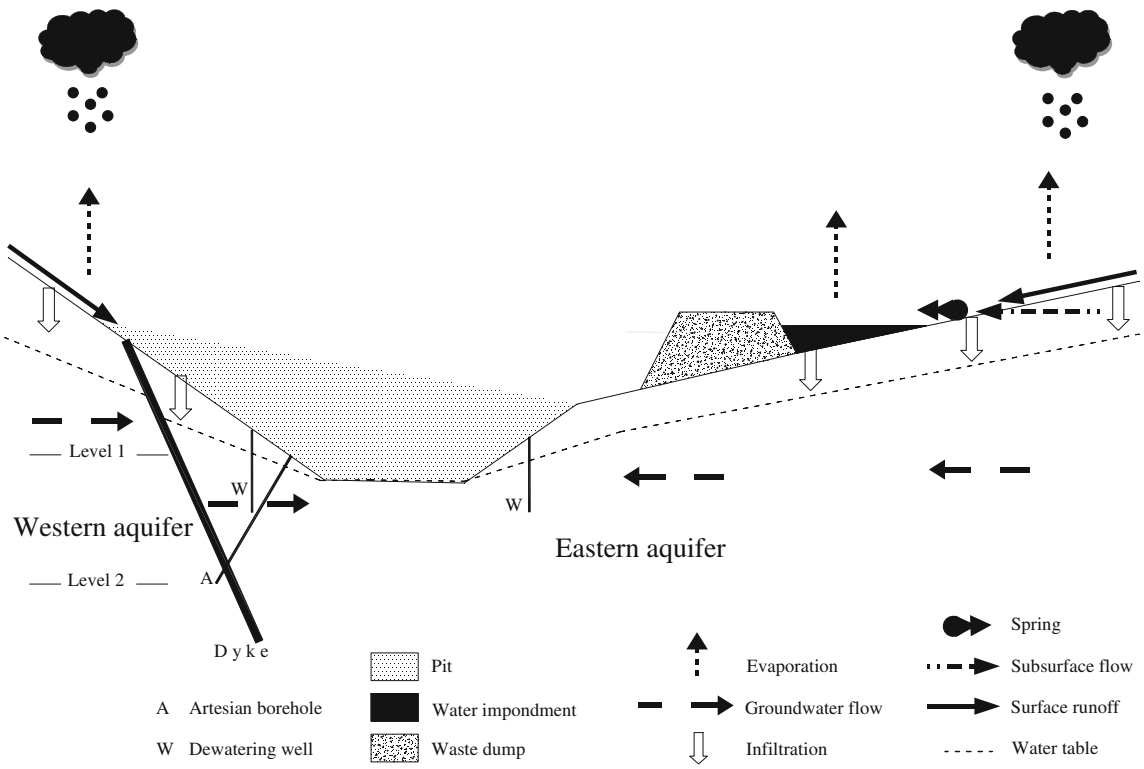

Fig. 11 Conceptual model of the study area (not to scale)

the origin of the artesian flow). Due to an average geothermal gradient of 3.2 °C/100 m, the depth difference between these two levels is most likely responsible for the water temperature difference between dewatering wells and artesian boreholes.

Conclusion

Stable and radioactive isotopes of water (^{18}O, ^{2}H, and ^{3}H) were analysed to help determine the recharge source and residence time of different water resources in the Sarcheshmeh copper mine area. Based on the isotopic composition of precipitation samples, the LMWL of the study area was established. The equation of this line is comparable to the LMWLs of other regions in Iran and neighbouring countries, reflecting the low humidity of the source region, but shows little effect from secondary evaporation during rainfall. Plotting of groundwater isotopic data on this line shows that both shallow and deep groundwater is meteoric in origin, although the deep groundwater has a longer residence time. Higher degrees of isotopic enrichment of shallow groundwater indicate that the major source was from surface runoff and ponded water (behind the waste dumps), which have undergone higher degrees of evaporation. Since this shallow groundwater system is currently responsible for most of the groundwater influx into the pit, reduction of its input by management of surface runoff and restriction of water ponding is recommended to reduce the wet working problems in the Sarcheshmeh copper mine pit. Reduction of input to the groundwater system, in addition to its economic benefits, can decrease the risk of mine flooding due to potential failure of the dewatering system.

Acknowledgments The authors thank the National Iranian Copper Industries Co. for funding this work. Part of this research was carried out when the second author visited the University of Waterloo, Canada. Constructive comments given by the Editor-in-Chief, the Associate Editor (Led Murray), and two anonymous reviewers are acknowledged.

References

Abbott MD, Lini A, Bierman PR (2000) $\delta^{18}O$, δD and ^{3}H measurements constrain groundwater recharge patterns in an upland fractured bedrock aquifer Vermont USA. J Hydrol 228:101–112

Abu-Jaber N, Kharabsheh A (2008) Ground water origin and movement in the upper Yarmouk basin, northern Jordan. Environ Geol 54:1355–1365

Acheampong SY, Hess JW (2000) Origin of the shallow groundwater system in the southern Voltaian Sedimentary Basin of Ghana: an isotopic approach. J Hydrol 233:37–53

Axel H (2006) Use of stable and radioactive isotopes and gaseous tracers for estimating groundwater recharge time of residence mixing of the different types of groundwater and origin in the Silao Romita aquifer Guanajuato central Mexico. Freiberg Online Geol, vol 17

Chen Z, Nie Z, Zhang G, Wan L, Shen J (2006) Environmental isotopic study on the recharge and residence time of groundwater in the Heihe River Basin northwestern China. Hydrogeol J 14:1635–1651

Clark ID, Fritz P (1997) Environmental isotopes in hydrogeology. Lewis Publication, Boca Raton

Cloutier V, Lefebvre R, Savard R, Bourque E, Therrien R (2006) Hydrogeochemistry and groundwater origin of the Basses-Laurentides sedimentary rock aquifer system St Lawrence Lowlands Quebec Canada. Hydrogeol J 14:573–590

Craig H (1961) Isotopic variations in meteoric waters. Science 133:1702–1703

Drimme RJ, Shouakar-Stash O, Walters R, Heemskerk AR (2001) Hydrogen isotope ratio of H_2O by automatic elemental analysis-continuous flow-isotope ratio mass spectrometry. Technical procedure 4.1, Rev 00. Environmental Isotope Laboratory, Department of Earth Sciences, University of Waterloo, Canada

Edmunds WM, Darling WG, Kinniburgh DG, Kotoub S, Mahgoub S (1992) Sources of recharge at Abu Delaig, Sudan. J Hydrol 131:1–24

Engle MA, Goff F, Jewett DG, Reller GJ, Bauman JB (2008) Application of environmental groundwater tracers at the Sulphur Bank Mercury Mine, California, USA. Hydrogeol J 16:559–573

Epstein S, Mayeda T (1953) Variation of ^{18}O content of waters from natural sources. Geochim Cosmochim Acta 4:213–224

Fantong WY, Satake H, Aka FT, Ayonghe SN, Asai K, Mandal AK, Ako AA (2010) Hydrochemical and isotopic evidence of recharge apparent age and flow direction of groundwater in the Mayo Tsanaga River Basin Cameroon: bearings on contamination. Environ Earth Sci 60:107–120

Faure G (1986) Principles of isotope geology. Wiley, New York

Friedman I, Machta L, Soiler R (1962) Water-vapor exchange between a water droplet and its environment. J Geophys Res 67:2761–2766

Gat JR (1971) Comments on the stable isotope method in regional groundwater investigations. Water Resour Res 7:980–993

Gat JR, Carmi I (1970) Evolution of the isotopic composition of atmospheric waters in the Mediterranean Sea area. J Geophys Res 75:3039–3048

Geirnaert W, Groenand M, Van der Sommen J (1984) Isotope studies as a final stage in groundwater investigations on the African shield. In: Challenges in African hydrology and water resources. IAHS publication, Harare, no 144, pp 141–153

Girard P, Hillaire-Marcel C, Oga MS (1997) Determining the recharge mode of sahelian aquifers using water isotopes. J Hydrol 197:189–202

Goni BI (2006) Tracing stable isotope values from meteoric water to groundwater in the southwestern part of the Chad basin. Hydrogeol J 14:742–752

Gupta H, Ray S (2007) Geothermal energy: an alternative resource for the 21st century. Elsevier, Amsterdam

Hamed Y, Dassi L, Tarki M, Ahmadi R, Mehdi K, Ben Dhia H (2011) Groundwater origins and mixing pattern in the multilayer aquifer system of the Gafsa-south mining district: a chemical and isotopic approach. Environ Earth Sci 63:1355–1368

Kazemi GA, Lehr JH, Perrochet P (2006) Groundwater age. Wiley-Interscience, New York

Khademi H, Mermut AR, Krouse HR (1997) Isotopic composition of gypsum hydration water in selected landforms from central Iran. Chemical Geol 138:245–255

Lee KS, Wenner DB, Lee I (1999) Using H and O isotopic data for estimating the relative contributions of rainy and dry season

precipitation to groundwater: example from Cheju Island Korea. J Hydrol 222:65–74

Leontiadis IL, Vergis S, Christodoulou TH (1996) Isotope hydrology study of areas in Eastern Macedonia and Thrace, Northern Greece. J Hydrol 182:1–17

Leybourne MI, Goodfellow WD (2007) Br/Cl ratios and O, H, C and B isotopic constraints on the origin of saline waters from eastern Canada. Geochim Cosmochim Acta 71:2209–2223

Leybourne MI, Clark ID, Goodfellow WD (2006) Stable isotope geochemistry of ground and surface waters associated with undisturbed massive sulfide deposits; constraints on origin of waters and water–rock reactions. Chemical Geol 231:300–325

Matter JM, Waber HN, Loew S, Matter A (2005) Recharge areas and geochemical evolution of groundwater in an alluvial aquifer system in the Sultanate of Oman. Hydrogeol J 14:203–224

Mohammadi Z (2006) Method of leakage study at karst dam sites, Zagros zone, Iran. PhD Thesis, University of Shiraz, Iran

Mohammadzadeh H (2010) The meteoric relationship for ^{18}O and ^{2}H in precipitations and isotopic compositions of water resources in Mashhad area (NE Iran). In: Proceeding of 1st international applied geological congress, Mashhad, Iran

Mohammadzadeh H, Ebrahimpoor S (2012) Application of stable isotope and hydrogeochemistry to investigate the origin and water resources quality variations in Zarivar lake catchment area. J Water Soil 26(4):1018–1041 (in Persian)

Morton KL, Mekerk FA (1993) A phased approach to mine dewatering. Mine Water Environ 12:27–34

Njitchoua R, Dever L, Fontes JC, Naah E (1997) Geochemistry origin and recharge mechanisms of groundwaters from the Garoua Sandstone aquifer, northern Cameroon. J Hydrol 190:123–140

Ortega-Guerrero A (2003) Origin and geochemical evolution of groundwater in a closed-basin clayey aquitard, northern Mexico. J Hydrol 284:26–44

Rose TP, Davisson ML, Hudson GB, Varian AR (1997) Environmental isotope investigation of groundwater flow in the Honey Lake basin, California and Nevada. Isotope Sciences Div, Lawrence Livermore National Lab, Livermore, CA, USA

Sahraei Parizi H, Samani N (2012) Geochemical evolution and quality assessment of water resources in the Sarcheshmeh copper mine area (Iran) using multivariate statistical techniques. Environ Earth Sci 69(5):1699–1718

Shahabpour J (1982) Aspects of alteration and mineralization at the Sarcheshmeh copper-molybdenum deposit, Kerman, Iran. PhD thesis, Leeds University, UK

Shahabpour J, Kramers JD (1987) Lead isotope data from the Sarcheshmeh porphyry copper deposit, Kerman, Iran. Miner Depos 22:278–281

SRK (2011) Sarcheshmeh copper mine open pit design; main report. SRK Consulting Ltd, Wales

Wassenaar LI, Athanasopoulos P, Hendry MJ (2011) Isotope hydrology of precipitation, surface and ground waters in the Okanagan Valley, British Columbia, Canada. J Hydrol 411(1):37–48